# Phosphorus recovery and recycling from model animal wastewaters using materials prepared from rice straw and corn cobs

Yifan Ding, David A. Sabatini and Elizabeth C. Butler

## ABSTRACT

Anthropogenic loss of phosphorus to surface waters not only causes environmental problems but depletes valuable phosphorus reserves. In this study, magnesium amended biochars and magnesium silicate, synthesized from corn cobs and rice straw, respectively, were evaluated for phosphorus uptake including the effects of pH and alkalinity. The overall goal was to close the phosphorus loop by recovering phosphorus from animal waste and reusing it as fertilizer. After phosphorus uptake, spent materials were tested for phosphorus release using modified soil tests representing different soil pH and alkalinity conditions. In experiments using model animal wastewaters containing both ammonia and bicarbonate alkalinity, dissolved phosphorus was removed by struvite ($MgNH_4PO_4 \cdot 6H_2O$) formation, whereas in deionized water, dissolved phosphorus was removed by adsorption. Alkalinity in the model animal wastewaters competed with phosphate for dissolved or solid-associated magnesium, thereby reducing phosphorus uptake. Spent materials released significant phosphorus in waters with bicarbonate alkalinity. This work shows that abundant agricultural wastes can be used to synthesize solids for phosphorus uptake, with the spent materials having potential application as fertilizers.

**Key words** | corn cobs, magnesium modified biochar, magnesium silicate, phosphorus reuse, rice straw

**Yifan Ding**
**David A. Sabatini**
**Elizabeth C. Butler** (corresponding author)
School of Civil Engineering and Environmental Science,
University of Oklahoma,
202 W. Boyd St., Room 334, Norman, OK, 73019-1024,
USA
E-mail: *ecbutler@ou.edu*

## HIGHLIGHTS

- Magnesium modified biochar and magnesium silicate were prepared from corn cobs and rice straw, respectively.
- These materials removed phosphorus from model wastewaters by struvite precipitation.
- Phosphorus uptake was limited by wastewater alkalinity.
- Spent materials released phosphorus under conditions mimicking calcareous soils.
- These materials show promise for phosphorus recovery and reuse.



doi: 10.2166/wst.2021.094

## GRAPHICAL ABSTRACT

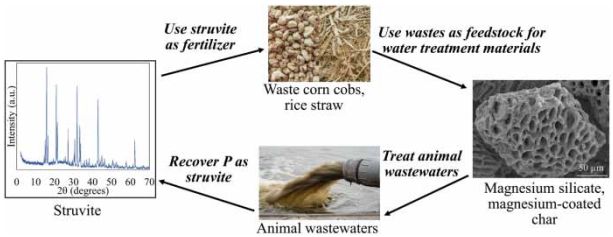


## INTRODUCTION

Phosphorus is introduced into the environment through runoff and seepage from agricultural activities such as crop and livestock production, as well as from municipal wastewater treatment plants and landfills (Nixon 1995). Not only does excess phosphorus introduction to surface waters cause eutrophication (Nixon 1995), it wastes a nutrient that is essential for agriculture and for which reserves of high-grade ores are limited (Roy 2017). In order to close the phosphorus cycle, therefore, efforts should be made not only to reduce consumption of new phosphorus ores, but also to recover and reuse phosphorus from wastes and wastewaters (Mukherjee *et al.* 2020; Withers *et al.* 2020). Potentially recoverable phosphorus from global livestock production waste is estimated to be 17.4 Mt per year, which could in theory meet 90% of the total phosphorus needed for agriculture (Kok *et al.* 2018). While animal manure has served directly as a fertilizer for centuries, it has several disadvantages, many of which also apply to composted manure or thermally treated biosolids. These include a phosphorus to nitrogen ratio greater than necessary for plant growth, which essentially wastes phosphorus when applied to soil, an unstable nitrogen content due to microbial denitrification, the potential for pathogen transmission, and aesthetic and regulatory concerns (Szogi *et al.* 2015; Bacelo *et al.* 2020). Recovery of phosphorus in a stable mineral form that can be easily stored and transported, as is studied here, is novel and poses an advantage over composted or thermally treated animal waste.

Phosphorus can be removed from wastewaters by precipitation as iron and aluminum phosphates, which results in formation of highly insoluble minerals that are unsuitable for use as fertilizers. Adsorption and precipitation using calcium-based (Mitrogiannis *et al.* 2017) and magnesium-based (e.g. Zhang *et al.* 2020) solids, on the other hand, yields solid phase phosphorus more suitable for use as fertilizer (e.g. Zhang *et al.* 2020). For instance, magnesium silicate minerals such as serpentine and chrysotile can effectively remove phosphate by interaction with $Mg(OH)_2$ surface groups (Smith & Hwang 1978), and layered double hydroxides can release dissolved $Mg^{2+}$ and $Ca^{2+}$ that can remove phosphorus by precipitation (Seida & Nakano 2002).

Nitrogen and phosphorus coexist in wastewaters, so their simultaneous precipitation as struvite ($MgNH_4PO_4{\cdot}6H_2O$) in the presence of dissolved $Mg^{2+}$ is commonly used to remove both. While struvite precipitation for phosphorus recovery is well established (Rittmann *et al.* 2011), it can be hindered by high ionic strength and bicarbonate alkalinity (Huchzermeier & Tao 2012), so phosphorus recovery as struvite should be tested in high ionic strength and high alkalinity wastewaters, as in this study.

Solution pH affects phosphorus uptake and subsequent release in several ways. First, it can strongly influence mineral surface charge, and therefore adsorption of charged species. For example, phosphate sorption to biochars with magnesium (hydr)oxide surfaces is favored at pH values below their $pH_{pzc}$ values, which range from 8.9 to 10.5 (Jiang *et al.* 2019), and sorption to magnesium silicate minerals is favored below their $pH_{pzc}$ values of 8.4–10.1 (Smith & Hwang 1978). Second, pH can strongly influence the tendency for phosphate removal by precipitation, by controlling the degree of protonation/deprotonation of cations (such as ammonium) and anions (such as $HPO_4^{2-}$). For instance, struvite solubility has a minimum around pH 9, due to acid-base equilibria among ammonia and phosphate species, with solubility increasing above and below this pH value (Hanhoun *et al.* 2011). At high pH values, hydroxide can compete with phosphate for magnesium to form $Mg(OH)_2(s)$ (Darwish *et al.* 2016).

A total of 144 million tons of corn cobs (Berber-Villamar *et al.* 2018) and 731 million tons of rice straw (Pinzi &

Dorado 2011) are produced globally each year. Such wastes have limited nutritional value for livestock (Khan *et al.* 2004), and the high silica content of rice straw makes it especially unsuitable as animal feed (Nakhshiniev *et al.* 2014). Fields are often cleared of crop residues by burning due to lack of low-cost alternatives (Ellis-Petersen 2019). For example, in Asia, 248 million tons of crop wastes are burned each year (Streets *et al.* 2003), leading to $CO_2$, $NO_x$, $SO_2$, and particulate emissions (Moraes *et al.* 2014).

As an alternative, crop wastes can be put to beneficial use as feedstock for novel water treatment materials. For example, crop wastes used to produce biochar can be amended with magnesium salts for phosphorus removal. To do this, wastes are typically treated with a soluble Mg salt, then pyrolyzed (Chen *et al.* 2018). During pyrolysis (>530 °C) solid $Mg(OH)_2$(s) on the biomass surface is transformed to MgO(s) (Choudhary *et al.* 1992). Since $Mg(OH)_2$(s) precipitation is favored at high pH (Huang *et al.* 2012), raising the solution pH when treating biomass with an Mg salt could yield a greater quantity of MgO after pyrolysis.

Agricultural wastes that are rich in silica (e.g. wheat husk, wheat straw, rice husk, and rice straw) can also be used to prepare magnesium silicate through extraction and dissolution of silica, followed by precipitation with $Mg^{2+}$ (Terzioglu & Yucel 2012). The term 'magnesium silicate' includes a series of minerals with different magnesium oxide and silica stoichiometric ratios, including chrysotile, olivine, and serpentine.

The overall goal of this study was to test two waste-produced materials, Mg-treated char and magnesium silicate, both synthesized in part from agricultural wastes, for their ability to uptake phosphorus and release it under varying conditions of pH and alkalinity. The specific objectives were: (1) to determine the optimum conditions, in terms of phosphorus uptake, for preparation of Mg-treated char and magnesium silicate, (2) to measure phosphorus uptake by these materials in simple model animal wastewaters containing both ammonia and carbonate, and (3) to measure phosphorus release from spent (post-phosphorus-exposure) materials under simulated soil pH conditions. Batch experiments were used to measure phosphorus uptake at a range of pH values and in the presence of both deionized water and two simple model animal wastewaters. Phosphorus release from spent materials was tested using modified soil extraction procedures to gain insight into the pH conditions favorable for phosphorus release and to understand the reactivity of solid associated phosphorus.

## MATERIALS AND METHODS

### Material characterization

Scanning Electron Microscopy (SEM) and Energy Dispersive X-ray Spectroscopy (EDS) were conducted using a JEOL JSM-840 scanning electron microscope at 20 kV coupled with Kevex X-ray analyzer or a Zeiss NEON 40 EsB scanning electron microscope at 15 kV and INCA Energy 250 Energy Dispersive X-ray Microanalysis system. Selected images are shown in the Supplementary material. X-ray Diffraction (XRD) was conducted using a Rigaku Ultima IV diffractometer with Cu-K-alpha radiation (40 kV, 44 mA). Data analysis was done with MDI JADE with the American Mineralogist Crystal Structure Database.

### Agricultural waste pretreatment

Agricultural wastes investigated include corn cobs (Kaytee, Chilton, Wisconsin), wheat straw (Thunder Acres, Conway Springs, Kansas), corn stalks (DriedDecor.com, West Jordan, Utah), wheat bran (Bob's Red Mill, Milwaukie, Oregon), pine shavings (Living World brand, Rolf C. Hagen Corp, Mansfield, Massachusetts), and rice straw (a mixture of *Oryza sativa* and *Tropical japonica*). The rice straw was donated by the Dale Bumpers National Rice Research Center, Stuttgart, Arkansas. First, all stalks or straw were cut using ceramic scissors to approximately 5 cm pieces and corn cobs were ground using a manual grain grinder (Azadx Model 500#, Amazon.com) to 0.125–0.180 mm (120–80 mesh). Next, biomass was washed in deionized (DI) water six times to remove residual soil. Then, biomass was soaked in 1 M $HNO_3$ (Certified ACS Plus, Fisher Chemical, Fair Lawn, New Jersey) for 30 minutes and rinsed with DI water until the rinsate reached pH 6. Finally, the biomass was oven-dried overnight at 60 °C.

### Preparation of Mg-amended biochars

A total of 15–30 g agricultural waste was placed in capped 100 mL porcelain crucibles and pyrolyzed in a programmable kiln (Caldera, Paragon Industries, Mesquite, Texas). Crucibles were capped to limit air exposure and thereby preserve carbon in the product. The temperature program was as follows: ramp at 300 °C per hour to 600 °C, isothermal at 600 °C for six hours, then cool naturally to room temperature (Ippolito *et al.* 2015; Brunson & Sabatini 2016). Initial experiments indicated that corn cobs had the highest mass

recovery of biochar (Table 1), so corn cobs were used for biochar preparation thereafter. Other chars with comparable mass recoveries, such as corn stalk char (Table 1), could not be readily separated from the aqueous phase due to physical properties or particle size, and interfered with phosphate spectrophotometric analysis.

All unamended chars contained negligible magnesium (Table 1), therefore corn cob biochar was augmented with magnesium in one of three ways (Supplementary material). In all cases, 30 g corn cobs was first soaked in 90 mL of a solution of 3.7 M $MgCl_2{\cdot}6H_2O$ (≥99%, Fisher Bioreagents, Ottawa, Ontario) with constant stirring. This was done in capped plastic bottles to reduce $CO_2$ dissolution from the atmosphere. 'Mg-char' was stirred for ten hours without pH adjustment (pH 6), oven dried at 60 °C, then pyrolyzed and used without further treatment (Supplementary material). 'Mg-char (pH 13, post-pyrolysis)' was prepared in the same way, except that after pyrolysis it was rinsed in a pH 13 solution of NaOH (ACS, EMD, Gibbstown, New Jersey) (Supplementary material). Finally, 'Mg-char (pH 13, pre-pyrolysis)' was stirred in a solution of 3.7 M $MgCl_2{\cdot}6H_2O$ at pH 6 for four hours, then adjusted to pH 13 by addition of NaOH pellets and stirred for another four hours, oven dried at 60 °C, and then pyrolyzed (Supplementary material).

All biochars were ground using a mortar and pestle, then sieved through a set of standard sieves (120 and 400 mesh) for 70 minutes on an electric sieve shaker (Houghton Manufacturing Co., Vicksburg, Michigan). Particles with diameters between 38 and 125 μm (400–120 mesh) were retained and used in the phosphorus uptake experiments.

## Preparation of magnesium silicate

Rice straw and wheat straw, both rich in silicon (Table 1) were pyrolyzed to obtain silicon-rich ash in a kiln using the same temperature program as above, but with uncapped crucibles to promote the oxidation and loss of carbon as $CO_2$, leaving only an inorganic, silicon-rich ash. A molar ratio of NaOH to Si of 2:1, based on the ash silicon content (Table 1), was used to dissolve the ash (Terzioglu & Yucel 2012). Specifically, 10 g rice straw ash was mixed with 590 mL of 0.64 M NaOH, or 2 g wheat straw ash was mixed with 50 mL of 0.64 M NaOH, both for three days with constant stirring. After this, the estimated dissolved Si concentration in both solutions, based on Table 1, was 0.32 M. The final pH values were 13.2 (rice straw ash) and 13.5 (wheat straw ash). Plastic bottles were used to avoid silica dissolution from glass and were kept closed to avoid dissolution of $CO_2$ from the atmosphere. Residual

**Table 1** | Pyrolysis yield and elemental composition of biochar and ash

| | Mass recovery and elemental composition[a] (wt %) | Rice straw | Wheat straw | Corn stalks | Corn cobs | Pine shavings | Wheat bran |
|---|---|---|---|---|---|---|---|
| Biochar[b] | Mass recovery | 14 | 7 | 14 | 16 | 10 | 7 |
| | C | 15 | 80 | 74 | 89 | 85 | 88 |
| | O | 36 | 18 | 17 | 11 | 15 | 12 |
| | Si | 48 | 1 | 6 | BDL[c] | 0 | BDL |
| | Mg | 0 | 0 | 0 | BDL | BDL | BDL |
| | P | 0 | 0 | 0 | BDL | BDL | 0 |
| | K | 0 | 0 | 2 | BDL | BDL | BDL |
| | Ca | 1 | 0 | 1 | 0 | 0 | BDL |
| Ash[d] | Mass recovery | 1 | 3 | 10 | 0 | 0 | 0 |
| | C | BDL | 6 | 21 | NM[e] | NM | NM |
| | O | 43 | 38 | 33 | NM | NM | NM |
| | Si | 53 | 23 | 19 | NM | NM | NM |
| | Mg | 0 | 2 | 2 | NM | NM | NM |
| | P | 0 | 0 | 1 | NM | NM | NM |
| | K | 0 | 23 | 14 | NM | NM | NM |
| | Ca | 2 | 1 | 5 | NM | NM | NM |
| | Cl | BDL | BDL | 4 | NM | NM | NM |
| | S | 1 | 7 | 2 | NM | NM | NM |

[a]Mass recovery = (mass after pyrolysis ÷ mass before pyrolysis) × 100%. Elemental composition was determined using scanning electron microscope-energy dispersive X-ray spectroscopy (SEM-EDS) with an estimated detection limit of 0.01 wt%.

[b]Biochar was produced by pyrolyzing biomass at 600 °C for six hours in capped crucibles, which limited oxygen supply.

[c]BDL: below detection limits.

[d]Ash was produced by pyrolyzing biomass at 600 °C for six hours in open crucibles.

[e]NM: not measured due to the low mass recoveries for ash from corn cobs, pine shavings, and wheat bran.

undissolved ash particles were filtered gravimetrically (Grade 1 filter paper, GE Healthcare Whatman, Fisher Scientific, Pittsburgh, Pennsylvania). Then, the remaining filtrate (approximately 590 mL for rice straw ash and approximately 50 mL for wheat straw ash) was added dropwise to an equal volume of 0.32 M $MgCl_2{\cdot}6H_2O$ to obtain an estimated Mg:Si molar ratio of 1:1 to precipitate magnesium silicate. The slurry was stirred for thirty minutes, then allowed to settle overnight. Then the supernatant was discarded and the solids were oven dried at 60 °C, then ground and sieved as described above.

## Phosphate analysis

For experiments with biochar, phosphate was quantified by Method 4500-P. E (Ascorbic acid method) (American Public Health Association 1992) using a Shimadzu UV-1601 spectrophotometer with a wavelength of 880 nm. Blanks containing sorbent materials (i.e. chars) but no phosphorus were tested in every experiment for absorbance at 880 nm due to scattering by fine particles or dissolved species that may have reacted with colorimetric reagents. No absorbance at 880 nm was found for these solid blanks in experiments with biochar. Therefore, in phosphate analysis for biochar samples, a blank containing neither solids nor phosphorus was placed in the reference cell of the spectrophotometer. For experiments with magnesium silicate, solid blanks (containing only magnesium silicate and no phosphorus) did have a small absorbance at 880 nm after reaction with the colorimetric reagents. This was most likely due to the presence of dissolved silica, which forms silicomolybdate (Chalmers & Sinclair 1966) with an intense blue color that absorbs at 880 nm and interferes with phosphate quantification. This was corrected by placing a solid blank, diluted in the same ratio as the samples, in the reference cell of the spectrophotometer.

In addition, to reduce the interference from silicate, a modified analysis method was used when quantifying phosphorus for experiments with magnesium silicate (Galhardo & Masini 2000). Addition of oxalic acid to the molybdate reagent prevents the formation of silicomolybdate, so that upon the later addition of the ascorbic acid reagent, the formed molybdenum blue is solely from phosphomolybdate (Galhardo & Masini 2000). In this modified method, the volume ratio of colorimetric reagents to sample was changed to 0.16:1 to maintain the same final molybdate concentration as in the ascorbic acid method (American Public Health Association 1992) and therefore to attain a similar degree of phosphate sensitivity. All other conditions, including the order of reagent addition and waiting times, were as reported elsewhere (Galhardo & Masini 2000).

## Model wastewater composition

In order to test the effect of ammonium/ammonia and bicarbonate alkalinity, phosphorus uptake was measured in two simple model systems representing wastewaters from production of swine and dairy cattle (Vanotti *et al.* 2003; Huchzermeier & Tao 2012). Concentrations in the model swine and cattle wastewaters were 24 mM total ammonia, up to 68.5 mg/L phosphate as P, and alkalinity values ranging from approximately 1,500 to 5,000 mg/L as $CaCO_3$ (Table 2).

## Phosphorus uptake experiments

Phosphorus uptake was measured in DI water as well as in the two model animal wastewaters. Solution pH was adjusted with 5 M HCl (Certified ACS Plus, Fisher Chemical, Fair Lawn, New Jersey) or 5 M NaOH (ACS, EMD Chemicals Inc., Gibbstown, New Jersey) before adding the solids and again before sampling. Isotherm batch tests contained 0.05 g or 0.075 g solid and 25 mL of DI or model wastewater (2 g/L or 3 g/L, respectively), with initial phosphate concentrations ranging from 0.7 to 68.5 mg P/L. Samples were equilibrated for 24 hours on a Cole-Parmer Ping-Pong TM #51504–00 shaker (Cole-Parmer, Vernon Hills, Illinois) at 60 excursions per minute, which was established as sufficient time for aqueous concentrations to reach a constant level (Supplementary material). All samples were prepared in duplicate.

After equilibration, reaction bottles were centrifuged at a relative centrifugal force of 3,661 × g for 30 minutes,

**Table 2** | Composition of the model wastewaters[a]

| Amount added | Model swine wastewater | Model cattle wastewater |
|---|---|---|
| $(NH_4)_2CO_3$ (mM) | 11.8 | 12.0 |
| $NaHCO_3$ (mM) | 23.6 | 84.5 |
| $NaH_2PO_4$ (as mg/L of P) | 68.5 | 68.5 |
| Resulting alkalinity (as mg/L of $CaCO_3$, considering ionic strength corrections[b]) | 1,535 (pH 7)<br>1,823 (pH 8)<br>1,955 (pH 9) | 4,605 (pH 7)<br>4,718 (pH 8)<br>4,997 (pH 9) |

[a]Chemicals and their sources were as follows: $NaHCO_3$ and $NaH_2PO_4$ (ACS, Fisher Chemical, Fair Lawn, New Jersey) and $(NH_4)_2CO_3$ (ACS, Alfa Aesar, Tewksbury, Massachusetts).
[b]Ionic strength corrections were calculated using MINEQL+ 5.0 (Environmental Research Software, Hallowell, Maine).

followed by filtration of a portion of the supernatant using 0.22 μm pore size hydrophilic polyvinylidene fluoride (PVDF) non-sterile syringe filters (Simsii Inc., Irvine, California) for phosphorus analysis (Section 2.5). After isotherm experiments, solids were separated from the remaining supernatant by gravity filtration (GE Healthcare Whatman Grade 5 qualitative filter paper), air dried, and kept in a desiccator for further analysis.

### Phosphorus release

After reaction with Mg-char or magnesium silicate, selected samples were tested for phosphorus release using three phosphorus extraction tests: Bray and Kurtz P1, Mehlich 3, and Olsen P (i.e. Estimation of available phosphorus in soils by extraction with sodium bicarbonate) (Bray & Kurtz 1945; Olsen 1954; Mehlich 1984), with the following minor modifications based on 'Methods of phosphorus analysis for soils, sediments, residuals, and waters' (Pierzynski 2000): (1) samples analyzed by the Bray and Kurtz P1 method were shaken for five minutes instead of one minute and (2) no charcoal was added to the samples for decolorization, since no color was observed. In addition, since these samples contained no soil, the solid to extracting solution ratio for all methods was adjusted to 1:800 (0.025 g solid was added to 20 mL of extracting solution) to better simulate the extractant to phosphorus ratio found in a soil test in which phosphorus is a minor constituent. Finally, the pH of the Mehlich 3 extracting solution (0.2 M $CH_3COOH$, 0.25 M $NH_4NO_3$, 0.015 M $NH_4F$, 0.013 M $HNO_3$, 0.001 M EDTA) was adjusted from 2.3 to 6.9 using $NH_4OH$ (ACS, 28.0–30.0% $NH_3$ basis, Sigma-Aldrich, St. Louis, Missouri) to simulate neutral soil water containing ligands that could compete with phosphate for adsorption sites. The extracting solutions for Bray & Kurtz P1 (0.03 M $NH_4F$ and 0.025 M HCl) and Olsen P (0.5 M $NaHCO_3$) had pH values of 2.5 and 8.4, respectively. After extraction, solids were removed using a 0.22 μm hydrophilic PVDF non-sterile syringe filter and phosphorus was measured as described above.

## RESULTS AND DISCUSSION

### Effect of pH on phosphorus uptake in DI water

Initial experiments with Mg-char (pH 13, post pyrolysis) and magnesium silicate made from rice straw were conducted in DI water at pH 7, 8, and 9 to identify the optimum pH for subsequent experiments. For both materials, there was more phosphorus uptake at pH 8 and 9 than at pH 7, particularly for Mg-char (pH 13, post pyrolysis) (Figure 1). There was not, however, a large increase in phosphorus uptake for either material upon changing the pH from 8 to 9 (Figure 1). This overall trend could be due to phosphate speciation, since between pH 7 and 8 there is a significant increase in the concentration of the divalent anion $HPO_4^{2-}$ due to deprotonation of $H_2PO_4^-$ ($pK_a = 7.2$), but a much smaller increase between pH 8 and 9. Electrostatic attractive forces are greater for divalent anions (e.g. $HPO_4^{2-}$) versus monovalent ions (e.g. $H_2PO_4^-$) of the same size (Valisko *et al.* 2007).

### Comparison of phosphorus uptake by different materials in DI water

A pH of 8 was selected for the comparison of the four chars (Supplementary material) since this pH value showed good uptake and was similar to that of animal wastewaters (Vanotti *et al.* 2003; Huchzermeier & Tao 2012). Unamended char showed very little capacity for phosphorus uptake at pH 8 (Figure 2(a), $Q_{e,max} = 1.4 \pm 0.5$ mg/g), which was attributed to the absence of magnesium (Table 3), and the Mg-char prepared without pH control ('Mg-char' in Supplementary material) also showed poor phosphorus uptake (Figure 2(a), $Q_{e,max} = 1.39 \pm 0.06$ mg/g). On the other hand, the $Q_{e,max}$ values of the two Mg-amended chars treated at pH 13 were $15.8 \pm 0.4$ and $31.9 \pm 0.7$ mg/g for post-pyrolysis and pre-pyrolysis, respectively (Figure 2(a)), which are ten to twenty times larger than Mg-char prepared without pH control. In addition, Mg-char (pH 13, pre-pyrolysis) removed $93 \pm 2$% of added phosphorus at the highest initial concentration of 68.5 mg P/L. Furthermore, this material had an isotherm characteristic of phosphorus uptake by precipitation (i.e. low uptake at low initial phosphorus concentrations, followed by a region where $Q_e$ values increased dramatically and the phosphorus $C_e$ values were independent of initial concentrations (Figure 2(a))). Phosphorus uptake on Mg-char (pH 13, post-pyrolysis), on the other hand, had an isotherm characteristic of adsorption (Figure 2(a)) similar to other reports (Jiang *et al.* 2019). The magnesium in the pH 13, pre-pyrolysis char may have been more soluble than that in the pH 13 post-pyrolysis char, facilitating phosphate removal by precipitation. Consistent with this, the pH 13 pre-pyrolysis char contained not only periclase (MgO(s)), but also the soluble magnesium salt bischofite ($MgCl_2 \cdot 6H_2O$) (Figure 3(a)).

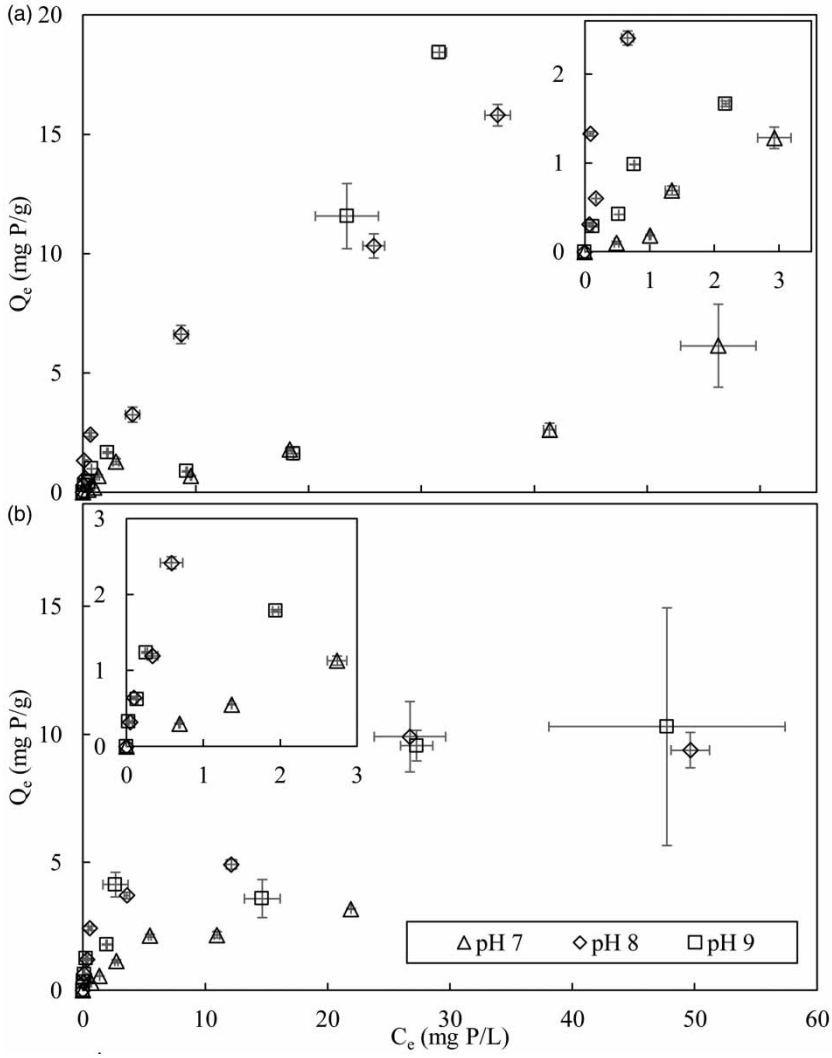


**Figure 1** | Phosphate removal by 2 g/L of (a) Mg-char (pH 13, post-pyrolysis) and (b) magnesium silicate synthesized from rice straw in DI water. The error bars show standard deviations of duplicate measurements.

The Figure 2(a) trend of increased phosphorus uptake by Mg-char (pH 13, post-pyrolysis, 28 wt % Mg (Table 3)) compared to the unamended char (no Mg (Table 3)) and Mg-char (10 wt% Mg (Table 3)) is likely due to greater precipitation of $Mg(OH)_2$(s) on the char matrix due to low solubility at very high pH. The better phosphorus uptake by Mg-char (pH 13, pre-pyrolysis, 9 wt % Mg) compared to Mg-char (10 wt % Mg), however, cannot be explained by magnesium mass concentration (Table 3), and could be due instead to the nature of the magnesium precipitate. At temperatures above 530 °C, the $Mg(OH)_2$(s) precipitated at high pH is transformed to MgO(s) (Choudhary *et al.* 1992). The powder XRD pattern of Mg-char (pH 13, pre-pyrolysis) correlates well with periclase (MgO(s), PDF# 98-000-0349) (specifically the peaks at 37.1°, 43.0°, and 62.4° 2$\theta$) (Figure 3(a)) confirming the conversion from $Mg(OH)_2$(s) to MgO(s) in the Mg-char (pH 13, pre-pyrolysis). The post-pyrolysis pH adjustment in the Mg-char (pH 13, post-pyrolysis), on the other hand, may have led to formation of a greater abundance of less soluble $Mg(OH)_2$(s), promoting uptake.

Magnesium silicate synthesized from rice straw showed better phosphorus uptake ($Q_{e,max} = 9.9 \pm 1.4$ mg/g) than magnesium silicate synthesized from wheat straw ($Q_{e,max} = 2.7 \pm 0.2$ mg/g, Figure 2(b)). In both cases, phosphorus uptake data fit well to the Freundlich isotherm (Figure 2(b)), suggesting that adsorption was primarily responsible for phosphorus uptake by these materials. Prior to phosphorus exposure, both magnesium silicates were poorly crystalline with similar XRD patterns that had

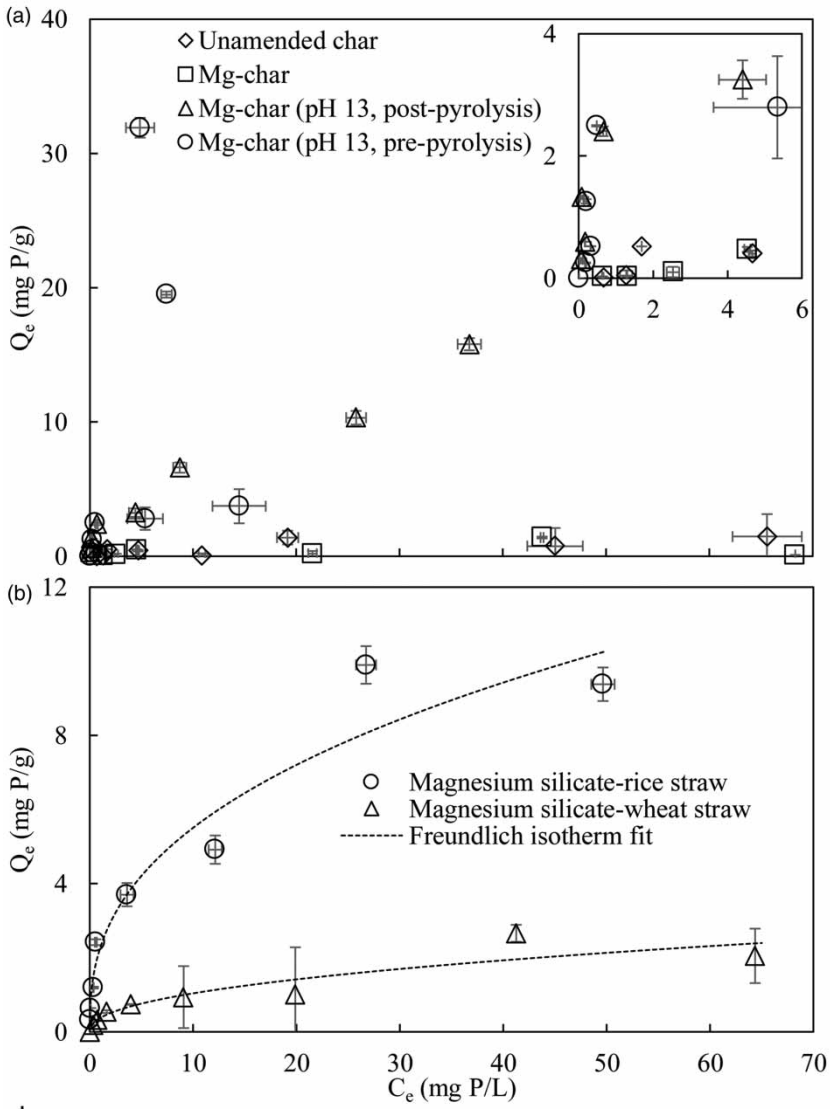


**Figure 2** | Phosphorus uptake by (a) biochars and (b) magnesium silicates in DI water with a solid concentration of 2 g/L at pH 8. The error bars show standard deviations of the means of $Q_e$ and $C_e$ values obtained from duplicate measurements. Freundlich isotherm parameters are $K = 0.37 \pm 0.13$; $n = 0.45 \pm 0.10$; $R^2 = 0.87$ and $K = 2.25 \pm 0.43$; $n = 0.39 \pm 0.06$; $R^2 = 0.95$ for magnesium silicate-rice straw and magnesium silicate-wheat straw, respectively. Uncertainties associated are standard errors. Freundlich parameters were calculated using nonlinear regression with the Levenberg Marquardt algorithm, using OriginPro 2017 (Origin Lab Corporation, Northampton, Maine).

broad peaks with 2$\theta$ values between approximately 20° and 30°, and at approximately 35° and 60° (Figure 4(a) and 4(b)). Fitting the XRD patterns with MDI JADE software identified antigorite ($Mg_{3-x}(Si_2O_5)(OH)_{4-2x}$, PDF# 00-002-0095) and enstatite ($MgSiO_3$, PDF# 98-000-6296) as possible magnesium silicate minerals with peaks in these regions.

The magnesium silicate synthesized from rice straw also had three narrow peaks (31.7°, 45.5°, and 56.4° 2$\theta$) corresponding to halite (NaCl) that likely formed from the presence of excess sodium (from NaOH) and chloride (from $MgCl_2{\cdot}6H_2O$) (Figure 4(a)). The XRD patterns for magnesium silicate from rice straw (Figure 4(a)) and wheat straw (Figure 4(b)) differed in the region below 10° 2$\theta$, with a larger peak centered at a lower value for magnesium silicate from wheat straw (Figure 4(b)) that could be explained by the presence of sepiolite ($Mg_4Si_6O_{23}H_{14}$, PDF# 98-002-0209) or vermiculite ($Mg_3Si_4O_{10}(OH)_2$, PDF# 98-000-1066). For magnesium silicate from rice straw, MDI JADE identified mutinaite ($SiO_2$, PDF# 98-001-1851) as a match for the broad peak around 10° 2$\theta$ (Figure 4(a)). The differences in magnesium silicate minerals present in the two materials may explain the differences in phosphorus uptake for the magnesium silicate prepared from rice straw and wheat straw (Figure 2(b)).

**Table 3** | Elemental analysis of corn cob biochars[a]

| Elements (wt %) | Unamended char | Mg-char | Mg-char (pH 13, post-pyrolysis) | Mg-char (pH 13, pre-pyrolysis) |
|---|---|---|---|---|
| C | 89 | 79 | 29 | 38 |
| Mg | BDL[b] | 10 | 28 | 9 |
| O | 11 | 9 | 34 | 28 |
| P | BDL | 0 | BDL | BDL |
| Cl | BDL | 2 | 8 | 20 |
| Na | BDL | BDL | 1 | 5 |

[a]Relative standard deviations for reported values are estimated to be 2–6% based on selected replicate measurements.
[b]BDL: below detection limit. The detection limit of EDS is approximately 0.01 wt %.

## Phosphorus uptake in simple model animal wastewaters

Next, the best performing materials from experiments in DI water (Mg-char (pH 13, pre-pyrolysis) and magnesium silicate-rice straw) were studied in simple model animal wastewaters containing both ammonia and carbonate alkalinity (Table 2). Experiments were conducted at both pH 8 and 9 due to better phosphorus uptake in DI water compared to pH 7 (Figure 1). These experiments were conducted with a solid concentration of 3 g/L to ensure sufficient magnesium for phosphorus uptake in the presence of competing ions such as bicarbonate.

The resulting uptake isotherms (Figure 5) did not correspond to a plateau shape typical of an adsorption isotherm where solute uptake is ultimately limited by surface functional groups for adsorption sites. Instead, the results are consistent with phosphate uptake by precipitation. Specifically, at low concentrations, $C_e$ is approximately equal to the initial added concentration ($C_0$), and $Q_e$ remains at approximately zero and is independent of $C_0$ (Figure 5). Then, above a threshold value of $C_0$, which likely corresponds to a solubility limit, $C_e$ becomes nearly independent of $C_0$ (it remains approximately constant) and all added solute is taken up by the solid, sharply increasing $Q_e$ (Figure 5). In such a system, the transition from the zone where $Q_e$ is independent of $C_0$ to that where $C_e$ is independent of $C_0$ corresponds to the point where the ion activity product equals the solubility constant of the mineral that controls solubility. While uptake of phosphorus by adsorption may also have taken place, trends in Figure 5 data indicate that precipitation was the predominant process

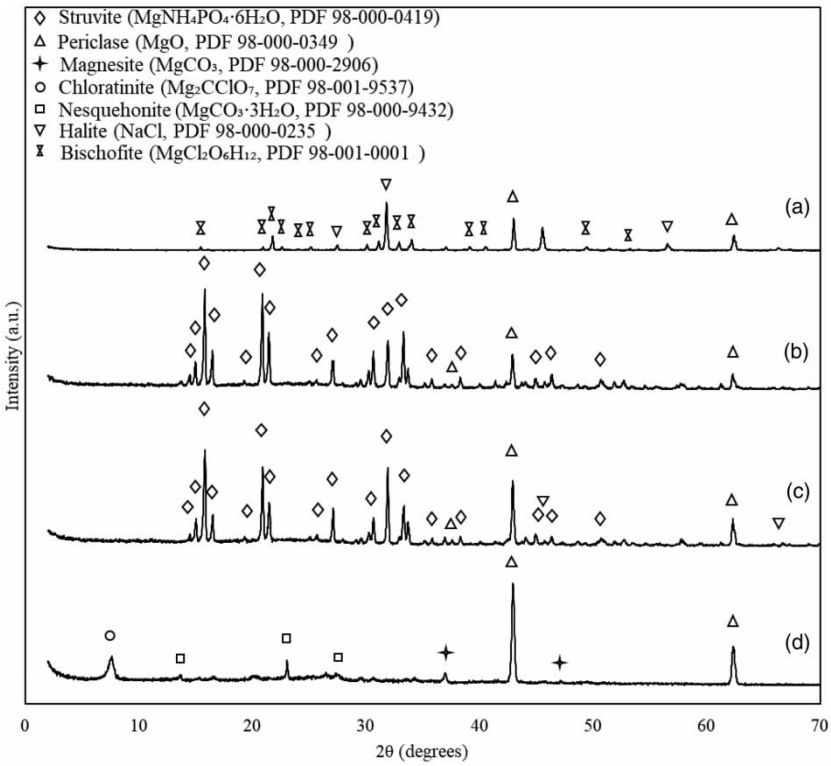


**Figure 3** | XRD patterns of Mg-char (pH 13, pre-pyrolysis) under the following conditions: (a) after synthesis and before exposure to any wastewater; (b) after exposure to pH 8 swine wastewater with phosphorus; (c) after exposure to pH 9 swine wastewater with phosphorus; and (d) after exposure to pH 8 swine wastewater without phosphorus.

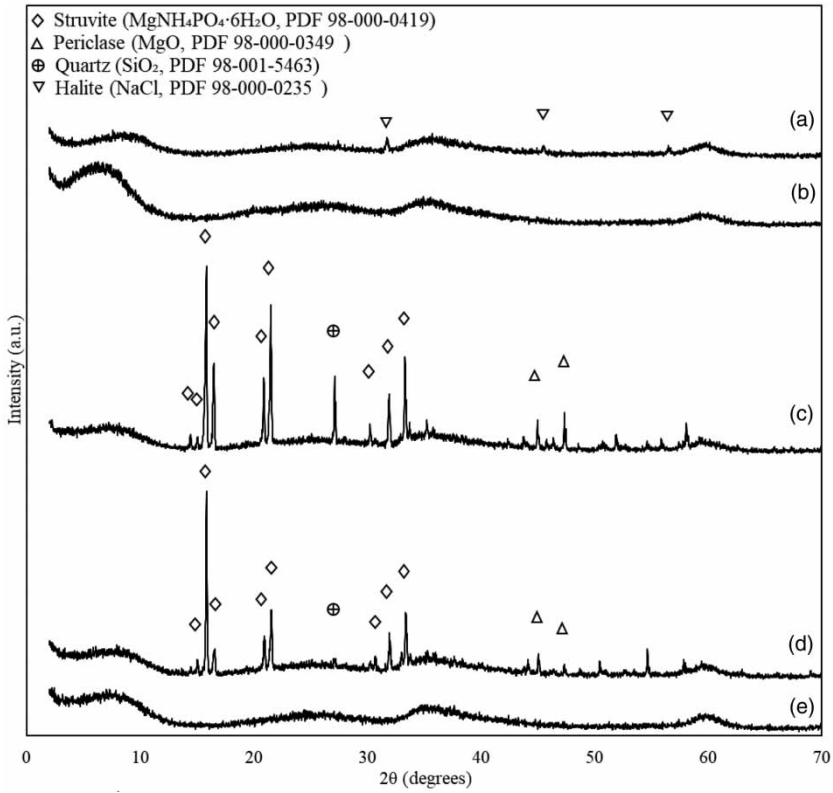


**Figure 4** | XRD patterns of magnesium silicate synthesized from rice straw and wheat straw. Patterns are: (a) magnesium silicate-rice straw and (b) magnesium silicate-wheat straw after synthesis and before wastewater exposure; magnesium silicate-rice straw after exposure to (c) pH 8 and (d) pH 9 model swine wastewater with phosphorus; (e) magnesium silicate-rice straw after exposure to pH 8 model swine wastewater without phosphorus.

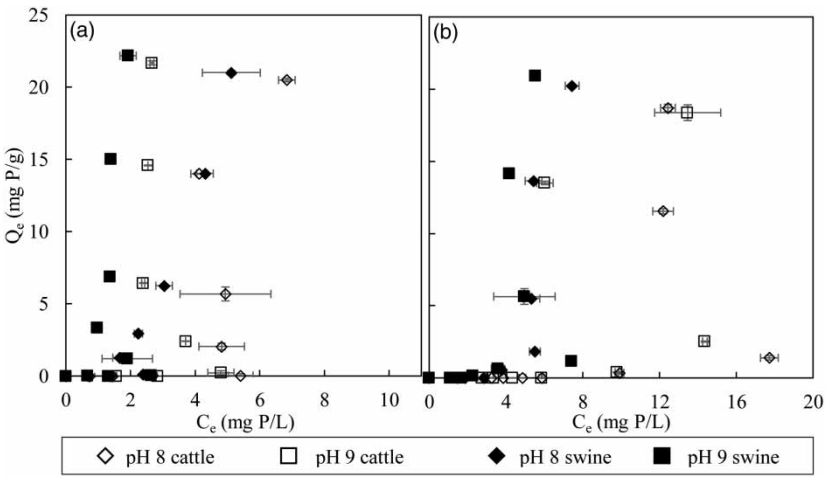


**Figure 5** | Phosphorus removal by 3 g/L of (a) Mg-char (pH 13, pre-pyrolysis) and (b) magnesium silicate synthesized from rice straw in model wastewaters. The error bars show standard deviations of duplicate measurements.

for phosphorus removal. XRD data indicate that the mineral struvite ($MgNH_4PO_4{\cdot}6H_2O$) was formed upon reaction of both Mg-char (pH 13, pre-pyrolysis) (Figure 3(b) and 3(c)) and magnesium silicate-rice straw (Figure 4(c) and 4(d)) with swine model wastewaters at both pH 8 and 9 (only one of the model wastewaters was chosen for XRD analysis.)

Several other phosphorus uptake trends were observed with model animal wastewaters. First, at higher concentrations where $C_e$ values were constant and independent

of added phosphorus concentration, Mg-char (pH 13, pre-pyrolysis) (Figure 5) achieved lower phosphate concentrations for each kind of wastewater at both pH 8 and 9 than magnesium silicate-rice straw (Figure 5). Another way of saying this is that the $C_e$ value where phosphorus concentration became independent of $C_0$ (likely due to precipitation) was lower for Mg-char (pH 13, pre-pyrolysis) than for magnesium silicate-rice straw (Figure 5). This could be due to a greater soluble concentration of $Mg^{2+}$ in equilibrium with char-associated $MgO(s)/Mg(OH)_2(s)$ versus magnesium silicate at pH 8 and 9, which would have the effect of increasing the struvite ion activity product above the solubility limit for a lower total concentration of phosphate.

Second, lower equilibrium concentrations of phosphorus were generally achieved at pH 9 (Figure 5, squares) versus pH 8 (Figure 5, diamonds), which may be due to the greater deprotonation of orthophosphate (i.e., more $HPO_4^{2-}$ versus $H_2PO_4^-$) at the higher pH value, which favors struvite formation (Darwish *et al.* 2016). Research has shown that pH values of 9 to 10 are most favorable for phosphorus recovery through struvite precipitation (Heraldy *et al.* 2017).

Finally, lower equilibrium concentrations were observed in the model swine wastewater compared to the model cattle wastewater. For example, for Mg-char (pH 13, pre-pyrolysis) at pH 9, lower $C_e$ values were obtained for the swine wastewater ($C_{e,max} < 3$ mg/L) versus the cattle wastewater ($C_{e,max} < 5$ mg/L) (Figure 5(a)). The same trend was observed for phosphorus uptake by magnesium silicate (Figure 5(b)). This can be explained by the significantly higher alkalinity in the model cattle wastewater (Table 2). Carbonate alkalinity likely competes with phosphate for dissolved $Mg^{2+}$, hindering phosphorus removal (Huchzermeier & Tao 2012). Evidence for this includes formation of the minerals magnesite ($MgCO_3$) and nesquehonite ($MgCO_3 \cdot 3H_2O$) on Mg-char (pH 13, pre-pyrolysis) that was equilibrated in model swine wastewater with no phosphorus (Figure 3(d)).

Despite the limitations discussed above, Mg-char (pH 13, pre-pyrolysis) and magnesium silicate made from rice straw removed a significant amount (97 and 92% of added 68.5 mg/L phosphorus, respectively) of the phosphorus present in pH 9 model wastewaters (Figure 5). Furthermore, the phosphorus uptake capacities measured in the model animal wastewaters (up to 22 mg/g, Figure 5) compare favorably to other studies of Mg amended biochars (30 mg/g (Chen *et al.* 2018) and 31 mg/g (Jiang *et al.* 2019)), considering the presence of significant alkalinity in the model wastewaters studied here. Furthermore, lowering the alkalinity prior to treatment for phosphorus uptake has the potential to significantly increase phosphorus removal efficiency (compare swine and cattle wastewaters (Figure 5(a) and 5(b)), which differ significantly in alkalinity (Table 2)). And although final $C_e$ concentrations in the treated animal wastewaters were higher than desirable for discharge to surface waters (8–14 mg/L, Figure 5), the sorbent materials produced in this study removed a significant fraction of the total added mass of phosphorus (up to 88%) for subsequent use as fertilizer. Since phosphorus concentrations significantly higher than the highest value studied here (68.5 mg/L as P) are common (e.g. Huchzermeier & Tao 2012), an even greater proportion of phosphorus could conceivably be recovered from animal wastewaters. In addition, treatment of such wastewaters with the materials synthesized here could be the first step in phosphorus removal that is aimed at phosphorus recovery for reuse, with subsequent treatment by, for example, advanced biological processes or precipitation with iron or aluminum salts, intended to achieve concentrations acceptable for discharge to surface waters. Important parameters to investigate in future research include the potential for formation of harmful byproducts in char, such as polynuclear aromatic hydrocarbons (Hale *et al.* 2012), as well as accumulation of metals, antibiotics, and antibiotic resistance genes in solids precipitated from animal waste (Cai *et al.* 2020).

## Release of phosphorus from spent materials

After exposure to phosphorus, Mg-char (pH 13, pre-pyrolysis) and magnesium silicate synthesized from rice straw were tested for phosphorus release using modified soil tests to mimic the spent material being applied as a fertilizer. Up to 55, 33, and 61 mg/g phosphorus was released using the Bray and Kurtz P1, modified Mehlich 3, and Olsen P procedures, respectively (Figure 6). The lowest phosphorus release in all cases was with the modified Mehlich 3 procedure, with significantly higher release being achieved with the Bray and Kurtz P1 and the Olsen P tests (Figure 6). In many cases, the Olsen-P test released more phosphorus than the Bray and Kurtz P-1. These trends suggest that a common process or processes are responsible for phosphorus release for both Mg-char (pH 13, pre-pyrolysis) and magnesium silicate-rice straw at both pH 8 and 9, consistent with the detection of struvite for both materials (Figures 3(b), 3(c), 4(c) and 4(d)).

The Bray and Kurtz P1 and the modified Mehlich 3 methods both employ $F^-$ (as $NH_4F$), which, like $HCO_3^-$ serves to displace sorbed phosphate (Dickman & Bray 1941).

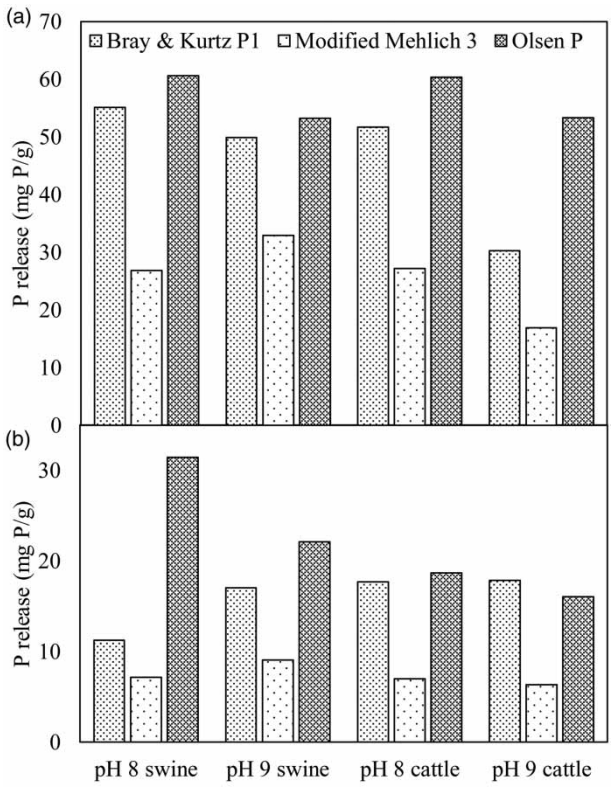


**Figure 6** | Phosphorus release by spent materials: (a) Mg-char (pH 13, pre-pyrolysis) and (b) magnesium silicate synthesized from rice straw. The final pH values of each extractant/solid mixture were 3.8–4.2 (Bray and Kurtz P1), 7.2–7.4 (Modified Mehlich 3), and 8.6 (Olsen P). The relative standard deviation ranged from 1–4% for measurements made in standard solutions of $NaH_2PO_4$.

Low pH serves to release acid-soluble phosphorus, or phosphorus in mineral form. In this study, the Mehlich 3 extracting solution was adjusted to neutral pH, whereas the Bray and Kurtz P1 extractant had a considerably lower pH. Under these conditions, the modified Mehlich 3 test likely released the concentration of adsorbed phosphorus and the Bray and Kurtz P1 estimated the sum of mineral and adsorbed phosphorus. Poor phosphorus release by the modified Mehlich 3 method suggests that precipitation was the dominant mechanism for phosphorus removal from the animal wastewaters.

The Olsen P extractant consists of 0.5 M $HCO_3^-$ (as $NaHCO_3$), which reacts with $Mg^{2+}$, driving dissolution of magnesium phosphorus minerals (Olsen 1954). Bicarbonate ($HCO_3^-$), like $F^-$, can also displace sorbed orthophosphate (Olsen 1954). Thus, the Olsen P test estimates concentrations of both solid ($HCO_3^-$ soluble) and sorbed orthophosphate. Good phosphorus release with the Olsen P test for both Mg-char (pH 13, pre-pyrolysis) and magnesium silicate from rice straw is also consistent with precipitation as the dominant phosphorus removal mechanism.

In some cases, the phosphorus released (Figure 6), expressed as mg P per g solid, exceeded phosphorus uptake (Figure 5, points with the largest $Q_e$ values (corresponding to $C_0 = 68.5$ mg P/L)). This can be explained by loss of significant sorbent mass during isotherm experiments (at least 50% in experiments with Mg-char (pH 13, pre-pyrolysis) and 6–13% in experiments with magnesium silicate-rice straw), most likely due to dissolution of soluble bishofite (Figure 3(a)) and halite (Figures 3(a) and 4(a)). Fine particles may also have been lost during solids retrieval after isotherm tests by centrifugation and filtration. Values of phosphorus uptake on the solids (i.e. $Q_e$ values in Figure 5) were calculated using the mass of solids added to the experiments, while values of released phosphorus (Figure 6) were calculated using the lower mass of solids retrieved from the isotherm experiments.

## CONCLUSIONS

Magnesium modified biochars prepared from corn cobs and magnesium silicate prepared from rice straw were tested for phosphorus recovery from simple model animal wastewaters containing ammonia and alkalinity. Char from corn cobs that was equilibrated with dissolved $Mg^{+2}$ at pH 13 prior to pyrolysis (Mg-char (pH 13, pre-pyrolysis)) showed the best phosphorus uptake. Precipitation of struvite was responsible for phosphorus uptake in the model wastewaters, and the best phosphorus removal was observed at pH 9, which was attributed to favorable phosphate speciation. Alkalinity in the model wastewaters significantly decreased phosphorus uptake through competition of bicarbonate and carbonate with phosphate for dissolved magnesium. After phosphorus uptake, spent materials were tested for phosphorus release using modified soil tests. Favorable levels of phosphorus release occurred from spent materials in the presence of bicarbonate (Olsen-P test), indicating the potential promise of these materials as fertilizers in calcareous soils.

The materials tested here are unique in that they are derived in part from agricultural wastes (corn cobs and rice straw) that are produced in large quantities each year, and that otherwise would be burned in the field in much of the world. Thus, diversion of these wastes for beneficial use avoids generation of pollutants such as $CO_2$, $NO_x$, and particulates that contribute to climate change ($CO_2$); tropospheric ozone, acidification, and eutrophication ($NO_x$); and direct health impacts (particulates). Furthermore, when applied to the soil as a phosphorus-enriched fertilizer, char

derived from agricultural wastes such as corn cobs also sequesters plant carbon in the soil, curbing $CO_2$ emissions. The magnesium in Mg-chars and magnesium silicate may also improve soil health. A more complete and accurate accounting of the environmental benefits and costs of the materials studied here, including water use, is needed. Issues of cost and sustainability will be addressed in future studies.

## ACKNOWLEDGEMENTS

The authors thank Andrew Elwood Madden for help with XRD analysis and Preston Larson for guidance with SEM-EDS analyses. Anna McClung and Laduska Sells at the USDA Dale Bumpers National Rice Research Center in Stuttgart, Arkansas kindly provided the rice straw used in this study. This work was supported by Agriculture and Food Research Initiative (AFRI) grant number 2018-67020-27805 from the USDA National Institute of Food and Agriculture.

## DATA AVAILABILITY STATEMENT

All relevant data are included in the paper or its Supplementary Information.

## REFERENCES

American Public Health Association 1992 *Standard Method 4500-P E: Ascorbic Acid Method*. APHA, Washington, DC.

Bacelo, H., Pintor, A. M., Santos, S. C., Boaventura, R. A. & Botelho, C. M. 2020 Performance and prospects of different adsorbents for phosphorus uptake and recovery from water. *Chemical Engineering Journal* **381**, 122566.

Berber-Villamar, N. K., Netzahuatl-Muñoz, A. R., Morales-Barrera, L., Chávez-Camarillo, G. M., Flores-Ortiz, C. M. & Cristiani-Urbina, E. 2018 Corncob as an effective, eco-friendly, and economic biosorbent for removing the azo dye Direct Yellow 27 from aqueous solutions. *Plos One* **13** (4), e0196428.

Bray, R. H. & Kurtz, L. 1945 Determination of total, organic, and available forms of phosphorus in soils. *Soil Science* **59** (1), 39–46.

Brunson, L. R. & Sabatini, D. A. 2016 Methods for optimizing activated materials for removing fluoride from drinking water sources. *Journal of Environmental Engineering* **142** (2), 04015078.

Cai, J., Ye, Z.-L., Ye, C., Ye, X. & Chen, S. 2020 Struvite crystallization induced the discrepant transports of antibiotics and antibiotic resistance genes in phosphorus recovery from swine wastewater. *Environmental Pollution* **266**, 115361.

Chalmers, R. A. & Sinclair, A. G. 1966 Analytical applications of $\beta$-heteropoly acids: this influence of complexing agents on selective formation. *Analytica Chimica Acta* **34**, 412–418.

Chen, Q. C., Qin, J. L., Cheng, Z. W., Huang, L., Sun, P., Chen, L. & Shen, G. Q. 2018 Synthesis of a stable magnesium-impregnated biochar and its reduction of phosphorus leaching from soil. *Chemosphere* **199**, 402–408.

Choudhary, V. R., Pataskar, S. G., Pandit, M. Y. & Gunjikar, V. G. 1992 Influence of precipitation conditions of magnesium-hydroxide on its thermal-decomposition in the preparation of active MgO. *Thermochimica Acta* **194**, 361–373.

Darwish, M., Aris, A., Puteh, M. H., Abideen, M. Z. & Othman, M. N. 2016 Ammonium-nitrogen recovery from wastewater by struvite crystallization technology. *Separation and Purification Reviews* **45** (4), 261–274.

Dickman, S. R. & Bray, R. H. 1941 Replacement of adsorbed phosphate from kaolinite by fluoride. *Soil Science* **52** (4), 263–274.

Ellis-Petersen, H. 2019 *The Guardian: Delhi's Smog Blamed on Crop Fires – but Farmers say They Have Little Choice*. Available from: https://www.theguardian.com/world/2019/nov/08/indian-farmers-have-no-choice-but-to-burn-stubble-and-break-the-law (accessed on 09-10-2020)

Galhardo, C. X. & Masini, J. C. 2000 Spectrophotometric determination of phosphate and silicate by sequential injection using molybdenum blue chemistry. *Analytica Chimica Acta* **417** (2), 191–200.

Hale, S. E., Lehmann, J., Rutherford, D., Zimmerman, A. R., Bachmann, R. T., Shitumbanuma, V., O'Toole, A., Sundqvist, K. L., Arp, H. P. H. & Cornelissen, G. 2012 Quantifying the total and bioavailable polycyclic aromatic hydrocarbons and dioxins in biochars. *Environmental Science & Technology* **46** (5), 2830–2838.

Hanhoun, M., Montastruc, L., Azzaro-Pantel, C., Biscans, B., Frèche, M. & Pibouleau, L. 2011 Temperature impact assessment on struvite solubility product: a thermodynamic modeling approach. *Chemical Engineering Journal* **167** (1), 50–58.

Heraldy, E., Rahmawati, F., Heriyanto & Putra, D. P. 2017 Preparation of struvite from desalination waste. *Journal of Environmental Chemical Engineering* **5** (2), 1666–1675.

Huang, X. H., Wu, T., Li, Y. J., Sun, D. J., Zhang, G. C., Wang, Y., Wang, G. P. & Zhang, M. L. 2012 Removal of petroleum sulfonate from aqueous solutions using freshly generated magnesium hydroxide. *Journal of Hazardous Materials* **219**, 82–88.

Huchzermeier, M. P. & Tao, W. D. 2012 Overcoming challenges to struvite recovery from anaerobically digested dairy manure. *Water Environment Research* **84** (1), 34–41.

Ippolito, J. A., Spokas, K. A., Novak, J. M., Lentz, R. D. & Cantrell, K. B. 2015 *Biochar for Environmental Management: Science, Technology and Implementation*. Routledge, Abingdon, Oxfordshire, pp. 139–163.

Jiang, Y. H., Li, A. Y., Deng, H., Ye, C. H., Wu, Y. Q., Linmu, Y. D. & Hang, H. L. 2019 Characteristics of nitrogen and phosphorus adsorption by Mg-loaded biochar from different feedstocks. *Bioresource Technology* **276**, 183–189.

Khan, M. A., Sarwar, M., Nisa, M.-u. & Khan, M. S. 2004 Feeding value of urea treated corncobs ensiled with or without enzose (corn dextrose) for lactating crossbred cows. *Asian-Australasian Journal of Animal Sciences* **17** (8), 1093–1097.

Kok, D. J. D., Pande, S., van Lier, J. B., Ortigara, A. R. C., Savenije, H. & Uhlenbrook, S. 2018 Global phosphorus recovery from wastewater for agricultural reuse. *Hydrology and Earth System Sciences* **22** (11), 5781–5799.

Mehlich, A. 1984 Mehlich 3 soil test extractant: a modification of Mehlich 2 extractant. *Communications in Soil Science and Plant Analysis* **15** (12), 1409–1416.

Mitrogiannis, D., Psychoyou, M., Baziotis, I., Inglezakis, V. J., Koukouzas, N., Tsoukalas, N., Palles, D., Kamitsos, E., Oikonomou, G. & Markou, G. 2017 Removal of phosphate from aqueous solutions by adsorption onto Ca(OH)(2) treated natural clinoptilolite. *Chemical Engineering Journal* **320**, 510–522.

Moraes, C. A., Fernandes, I. J., Calheiro, D., Kieling, A. G., Brehm, F. A., Rigon, M. R., Berwanger Filho, J. A., Schneider, I. A. & Osorio, E. 2014 Review of the rice production cycle: by-products and the main applications focusing on rice husk combustion and ash recycling. *Waste Management & Research* **32** (11), 1034–1048.

Mukherjee, D., Ray, R. & Biswas, N. 2020 In: *Sustaining Resources for Tomorrow* (J. A. Stagner & D. S. K. Ting, eds). Springer International Publishing, Cham, Switzerland, pp. 67–81.

Nakhshiniev, B., Biddinika, M. K., Gonzales, H. B., Sumida, H. & Yoshikawa, K. 2014 Evaluation of hydrothermal treatment in enhancing rice straw compost stability and maturity. *Bioresource Technology* **151**, 306–313.

Nixon, S. W. 1995 Coastal marine eutrophication: a definition, social causes, and future concerns. *Ophelia* **41** (1), 199–219.

Olsen, S. R. 1954 *Estimation of Available Phosphorus in Soils by Extraction with Sodium Bicarbonate*. Circular No. 939, US Department of Agriculture. Available from: https://books.google.com/books?hl=en&lr=&id=d-oaM88x5agC&oi=fnd&pg=PA2&ots=zZVm_DeVYF&sig=_pYkPW6dJUmRnXocoRGFbfo500k#v=onepage&q&f=false (accessed on 22-12-2020)

Pierzynski, G. M. 2000 *Methods of Phosphorus Analysis for Soils, Sediments, Residuals, and Waters*. Southern Cooperative Series Bulletin No. 396, Kansas State University, Manhattan, KS, USA. Available from: http://citeseerx.ist.psu.edu/viewdoc/download?doi=10.1.1.606.5702&rep=rep1&type=pdf (accessed on 22-12-2020)

Pinzi, S. & Dorado, M. P. 2011 In: *Handbook of Biofuels Production* (R. Luque, J. Campelo & J. Clark, eds). Woodhead Publishing, Duxford, Cambridgeshire, pp. 61–94.

Rittmann, B. E., Mayer, B., Westerhoff, P. & Edwards, M. 2011 Capturing the lost phosphorus. *Chemosphere* **84** (6), 846–853.

Roy, E. D. 2017 Phosphorus recovery and recycling with ecological engineering: a review. *Ecological Engineering* **98**, 213–227.

Seida, Y. & Nakano, Y. 2002 Removal of phosphate by layered double hydroxides containing iron. *Water Research* **36** (5), 1306–1312.

Smith, R. W. & Hwang, M.-Y. 1978 Phosphate adsorption of magnesium silicates. *Journal – Water Pollution Control Federation* **50** (9), 2189–2197.

Streets, D., Yarber, K., Woo, J. H. & Carmichael, G. 2003 Biomass burning in Asia: annual and seasonal estimates and atmospheric emissions. *Global Biogeochemical Cycles* **17** (4), 10–20.

Szogi, A. A., Vanotti, M. B. & Ro, K. S. 2015 Methods for treatment of animal manures to reduce nutrient pollution prior to soil application. *Current Pollution Reports* **1** (1), 47–56.

Terzioglu, P. & Yucel, S. 2012 Synthesis of magnesium silicate from wheat husk ash: effect of parameters on structural and surface properties. *Bioresources* **7** (4), 5435–5447.

Valisko, M., Boda, D. & Gillespie, D. 2007 Selective adsorption of ions with different diameter and valence at highly charged interfaces. *The Journal of Physical Chemistry C* **111** (43), 15575–15585.

Vanotti, M. B., Szogi, A. A. & Hunt, P. G. 2003 Extraction of soluble phosphorus from swine wastewater. *Transactions of the Asae* **46** (6), 1665–1674.

Withers, P. J. A., Forber, K. G., Lyon, C., Rothwell, S., Doody, D. G., Jarvie, H. P., Martin-Ortega, J., Jacobs, B., Cordell, D., Patton, M., Camargo-Valero, M. A. & Cassidy, R. 2020 Towards resolving the phosphorus chaos created by food systems. *Ambio* **49** (5), 1076–1089.

Zhang, T., He, X., Deng, Y., Tsang, D. C., Yuan, H., Shen, J. & Zhang, S. 2020 Swine manure valorization for phosphorus and nitrogen recovery by catalytic–thermal hydrolysis and struvite crystallization. *Science of the Total Environment* **729**, 138999.

First received 28 October 2020; accepted in revised form 27 February 2021. Available online 10 March 2021